Quantitative Assessment of Bone Mineral Content in Dental Radiogram

Takenori Noikura

Department of Dental Radiology
Kagoshima University Dental School
8-35-1 Sakuragaoka, Kagoshima 890-8544, Japan

Abstract:

Aluminum Equivalent (AL equivalent) image system was developed to measure the bone mineral content in mandible using conventional dental radiography, intraoral digital dental radiography and panoramic radiography by one shot dual energy subtraction method. Z-score was used as evaluation of bone changes, because of variation of normal mandibular bone of AL equivalent values by age, gender and region.

For clinical application, Z-score was taken to evaluate of periapical bone changes after root canal treatment, bone changes in the around of implant, bone changes in elderly subjects, and bone changes of end stage of renal diseases. Furthermore, for application of animal experiments, AL-equivalent values were used to evaluate the effect of microgravity to the vertebral growth in growing rats, and effects on the bone mineral content by himdlimb suspension in rats.

Key words:

Aluminum equivalent image, panoramic energy subtraction,
mandible bone changes, the effect of microgravity to vertebral bone

I. Preface

Various kinds of devices such as QCT and DEXA have been developed to measure bone mineral content for medical examination and treatment[1, 2]. However, it is quite difficult to adapt these devices to the jawbone. Therefore, dental radiogram was used to measure the bone mineral content in the jawbone. It is well known that aluminum (Al) or copper (Cu) step can be radiographed simultaneously and converted to Al or Cu equivalent value for quantitative analysis, which was used for densitometric measurement by optical density scanning[3, 4]. However, these calculations were time consumption and not practical for clinical application.

We developed a computer-processing system[5] to convert equivalent image using aluminum as a reference for intraoral dental radiography, intraoral digital radiography and panoramic radiography. As the equivalent value is indicated by X-ray attenuation according to aluminum thickness, it provides a value corresponding to the quantity of bone mineral content. Furthermore, the precision of aluminum equivalent value

obtained allows longitudinal comparison, that is, it was able to demonstrate not the absolutely quantity of bone mineral content, but relative changes.

For clinical applications, mandibular bone changes were examined in the periapical regions, around implants, in elderly subjects, and in renal osteodystrophy in which was suggested in elucidation on bone metabolism of VD_3. In an animal experiments, this method was used to examine the effect of a 14 days space-flight on the vertebrae of a rat. In further animal experiments, changes in bone mineral content of rat femur following suspension.

II. Fundamental study for bone mineral content of mandible

A. System of AL Equivalent system

The aluminum equivalent imaging system consists of dental film, TV-camera, Computer processing system and display. Data was input using a TV system and digitized to 8 bit density. The aluminum equivalent value was calculated by a cubic conversion curve to the gray level of the wedge. Equivalent image was newly presented as the density axis using the aluminum equivalent value, and displayed as either a black and white, or color image (Fig.1).

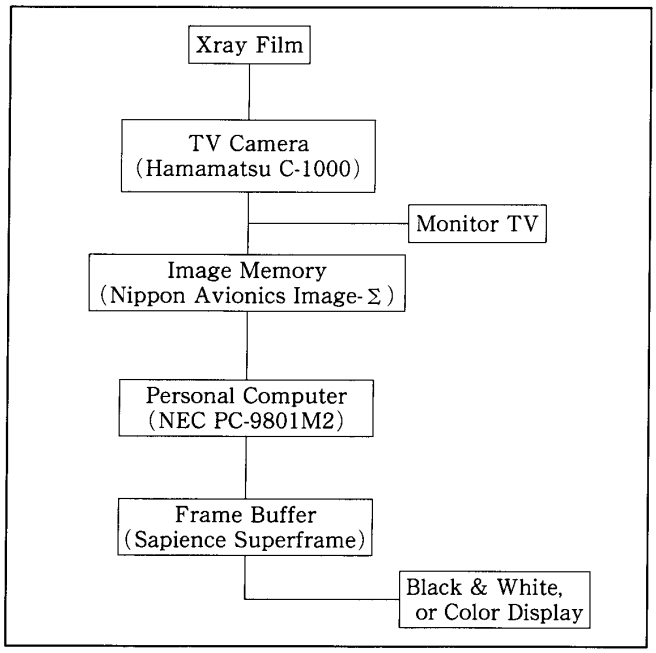

Fig. 1 Block Diagram of Al Equivalent System

B. Indicator and aluminum wedge

An aluminum wedge for reference was attached to the indicator, and radiographed together on the dental film. The shape of reference was designed for easy input of the data into the computer using a wedge instead of a step. The thickness of the aluminum wedge varied from 0 mm to 16mm, and set with an indicator, that was radiographed on the dental film (Fig.2).

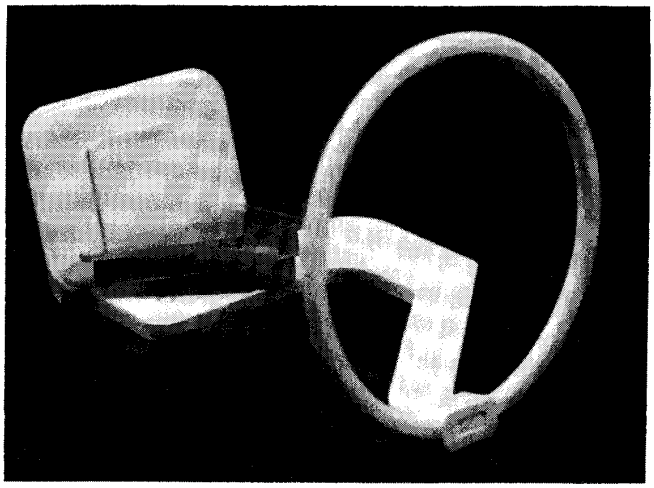

Fig. 2 Indicator with aluminum wedge

C. Intraoral dental radiography

Dental radiogram was used to obtain aluminum equivalent image. As a reference, aluminum was adopted because it shows an attenuation coefficient similar to that of bone. Film was processed as film to the usual in an automatic developing machine (Fig.3-1).

Fig. 3-1 Dental Radiogram

A TV system (C1000, Hamamatsu Photonics) was used for inputting of images. The TV system is capable of high-speed input of plane data, but is still inferior to a laser or drum scanner in noise and

dynamic range. Therefore, digitalization is performed at a resolution of 8 bits after reducing the image noise and light source fluctuation to 1/16 (theoretical value) by 256-time digital integration and averaging for maximum use of the film density and luminance values (Image-Σ Nippon Avionics Co., Ltd.). The brightness data were converted to aluminum equivalent values by preparing a cubic or quadratic polynomial conversion curve based on the data of a reference material (aluminum) and are displayed as aluminum equivalent images using a color scale with a frame buffer (Super Frame, Sapience). This aluminum equivalent value is line integral of X-ray attenuation in the entire distance from the X-ray tube to the film converted to the length of aluminum. The range of conversion corresponds to a 0-16mm range of aluminum thickness. What is important here is that the values obtained are equivalents of aluminum X mm with a dimension of square density (Fig.3-2).

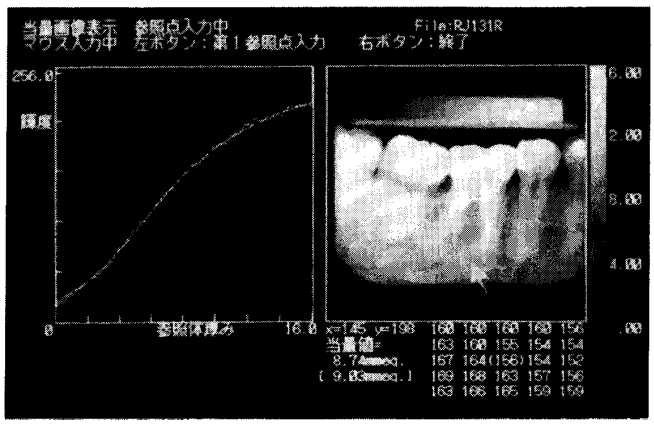

Fig. 3-2 Al-Equivalent Image

1. Precision and accuracy

Equivalent values were obtained using steps of aluminum thickness from 2 mm to 16mm. Accuracy and precision were 5.6% and 3.8% respectively in this system.

2. Conversion of Al-Eq value to $CaCO_3$ (mg/cm^2)

Conversion of aluminum equivalent values to calcium carbonate values for comparison with the results of other bone mineral measurement methods was evaluated. Urethane containing $CaCO_3$ at known concentrations was used as $CaCO_3$ phantoms for the bone mineral measurement (Kyoto Kagaku, UCA model). Aluminum equivalent values of 9 blocks containing $CaCO_3$ at 461.2 mg/cm^3 to 939 mg/cm^3 were determined, and a conversion curve of aluminum equivalent values to $CaCO_3$ values in mg/cm^3 was prepared. The dimension used in this conversion was the square density (g/cm^2) obtained by multiplying the aluminum density value by the specific gravity of aluminum (2.7 g/cm^3) or by multiplying the $CaCO_3$ density by the thickness of the phantom block (1 cm). Since the aluminum equivalent values of the $CaCO_3$ phantoms included those of urethane, X-ray attenuation by urethane was assumed to be equal to that by soft tissue, and the conversion curve was considered to be one for the bone-soft tissue complex. The two parameters were linearly correlated, and the aluminum equivalent value of urethane, corresponding to the matrix of bony tissue, is expressed as the intercept on the Y axis ($X = 0$).

B. Intraoral digital dental radiography

Recent intraoral digital dental radiography[6, 7], in which CCD and photostimulable fluorescent materials are used, has enabled immediate imaging unlike conventional film radiography, facilitated image transfer and storage by digitalization, and reduced the exposure, and its clinical application is attempted because of these merits. However, the thickness of the sensor, a narrow imaging area, and an inferior spatial resolution compared with dental films are its disadvantages. Particularly, because the pixel value of digital images is often linearly related to the dose, the images give the impressions that they have a narrow dynamic range and look different from conventional X-ray images, which we have been accustomed to. Also, the variation in the tone among models of the apparatus may lead to confusion in future. The aluminum equivalent method provides visually satisfactory digital X-ray images and equalizes the tone among different apparatuses or film images. In the intraoral digital radiographic system Dixel (MCR-1000, Morita Corp., Kyoto) used in this study, the sensor is a CCD

(charge-coupled device), and the X-ray generator is MAX-F1 (Morita Corp., Kyoto) at a tube voltage of 60 kV, a tube current of 10 mA, and a total filtration of Al 1.5 mm and is synchronized with the electronic shutter of CCD. The pixel number of the CCD is 400 x 600, the size of a single pixel is 48 x 48 μm , and the number of tones is 256 (8 bit). Image files are stored in magnet-optical discs. An image file consists of a header and a data portion. Data of the circumstances of radiography (patient information, date, time) are recorded in the text format in the header, and image data are recorded in the 1 byte/pixel binary format in the data portion. Image files were converted to the BMP format (standard image format) by Visual BASIC (Microsoft Corp., USA) of Windows using a personal computer (PC9821, NEC), these images were displayed, and the pixel values were determined. For equivalent imaging, an Al-wedge (0-16 mm thick) was attached as a reference to the indicator with a sensor (Fig.4-1, 2).

Fig. 4-1 Dixel Imaging System

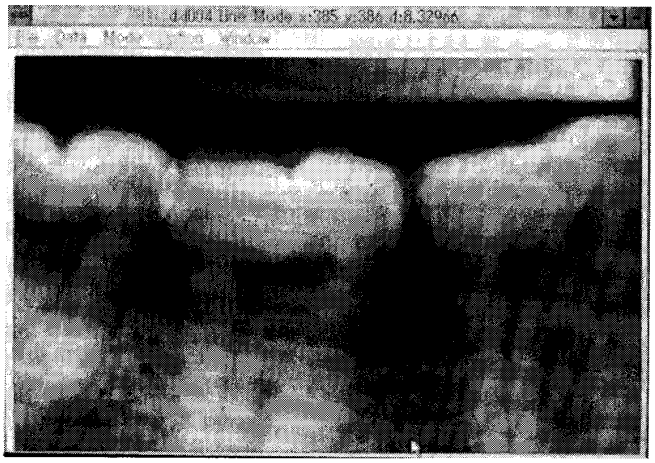

Fig. 4-2 Al Equivalent Image by Dixel radiography

C. Panoramic radiography using energy subtraction method

Measurement of bone mineral content by one-shot dual energy subtraction of panoramic radiography was performed. For separating the bone mineral content from soft tissue on panoramic images, a one-shot dual energy subtraction method[8, 9, 10] was employed by using computed radiography (CR-7000) and CR-workstation. The tube voltage was 80KVp with Sm-filter. Cu-filter of 0.4mm thickness was set between the first and the second imaging plate (IP). As references, aluminum cylinders (3-12mm) and aluminum wedge (2-18mm) which was theoretically created corresponding to tomographic image layer were put in water phantom, and set on chin-rest. The subtraction images were evaluated by $CaCO_3$ with urethane (standard Phantom), and compared with aluminum equivalent images of dental films. Aluminum equivalents of the $CaCO_3$ blocks as references in water radiographed on plane image were corresponded to panoramic subtraction images. Aluminum equivalents of $CaCO_3$ phantoms were separated form urethane as soft tissue by panoramic subtraction images. On the patient, panoramic subtraction images showed lower than dental aluminum equivalent images because of soft tissue, which were estimated about 20-30% content of soft tissue (Fig. 5-1, 2, 3, 4).

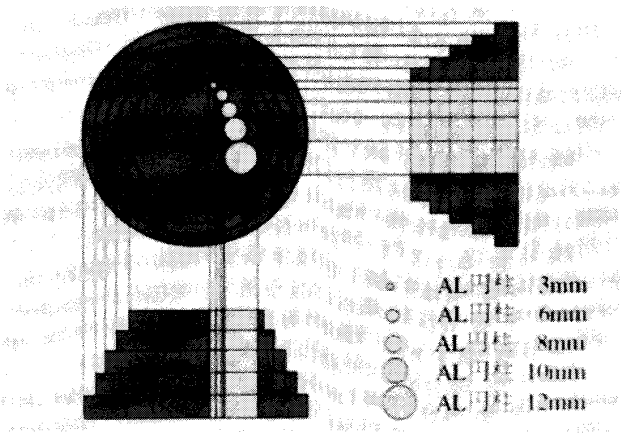

Fig. 5-1 Phantom for Energy Subtraction

Fig. 5-2 Subtraction Bone Image by Panoramic Radiography

Fig. 5-3 Subtraction Soft Tissue Image by Panoramic Radiography

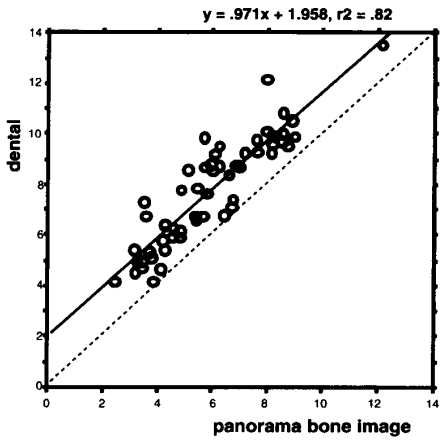

Fig. 5-4 Comparison AL-Eq value between Energy subtraction image and Dental image

D. Evaluation of bone changes by aluminum equivalent images

1. Data sampling area and aluminum equivalent values of normal mandibular bone

Data sampling area was located at each alveolar septum of the mandibular premolar and molar regions by a range that does not exceed half the root length to avoid influence.

The mean and SD of aluminum equivalent values in normal alveolar septum of mandibular premolar and molar regions (Fig.6-1, 2).

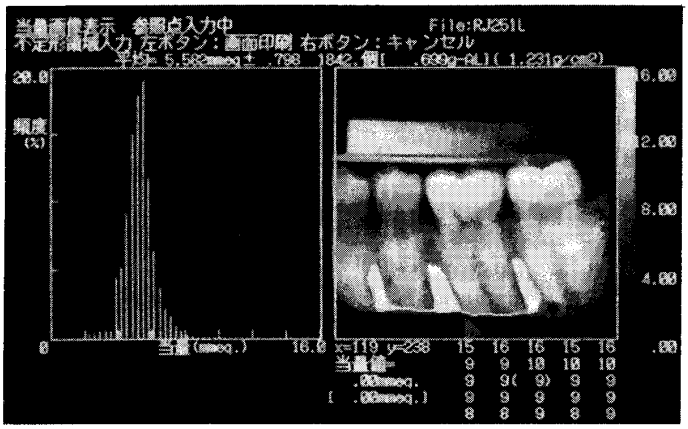

Fig. 6-1 Data Sampling Area and Aluminum Equivalent Values of Normal Mandibular Bone.

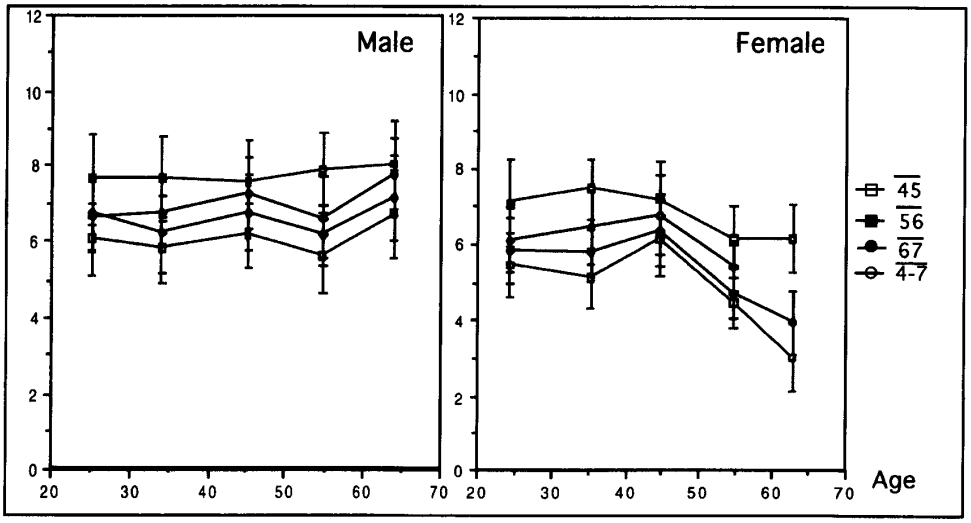

Fig. 6-2 The Mean and SD of Aluminum Equivalent Values in Alveolar Septum of Mandibular premolar and molar regions in Normal subjects.

2. Evaluation of bone changes by Z-score

Because Al equivalent value of normal mandibular bone changes by age, gender and region, bone changes were evaluated by normalization to the Z-score in the normal group. Z-score is calculated following a numerical formula. As the fundamental criterion for evaluation of bone changes, Z-score is based on ±2 SD.

$$\text{Z-score} = \frac{\text{Sample Al-Eq} - \text{Ave. AL-Eq (normal)}}{\text{SD of Ave. AL-Eq (normal)}}$$

III. Clinical application

A. Periapical bone changes after root canal treatment

Periapical bone changes are usually observed as normal, radiolucent or radiopaque areas on radiograms. Here, differences between such macroscopic findings and equivalent image were compared. Furthermore, those relations to the condition of root canal fillings were examined. Periapical bone changes on radiograms were compared to analysis of Z-score of aluminum equivalent images. There were 1370 teeth used for evaluation. Bone changes of the root apices were divided into 3 groups by radiographic findings as normal, radiolucent or radiopaque. Al equivalent values were obtained from a sampling area at each root apex and evaluated by the Z-score from a normal root apex (Fig.7-1). Findings were divided

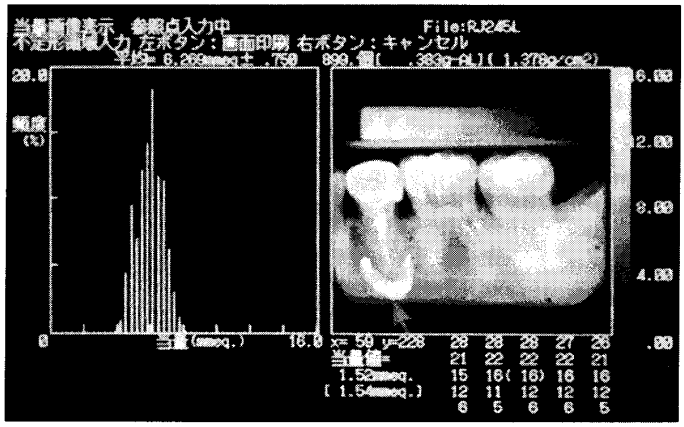

Fig. 7-1 Periapical Bone Changes after root canal treatment

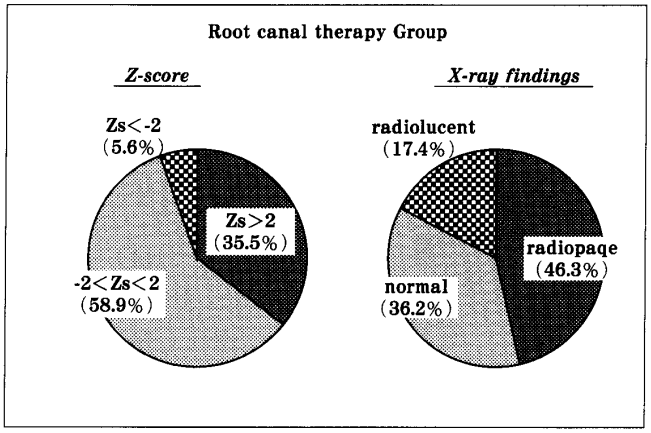

Fig. 7-2 Difference of Evaluation between Z-score and X-ray findings at Periapical Regions

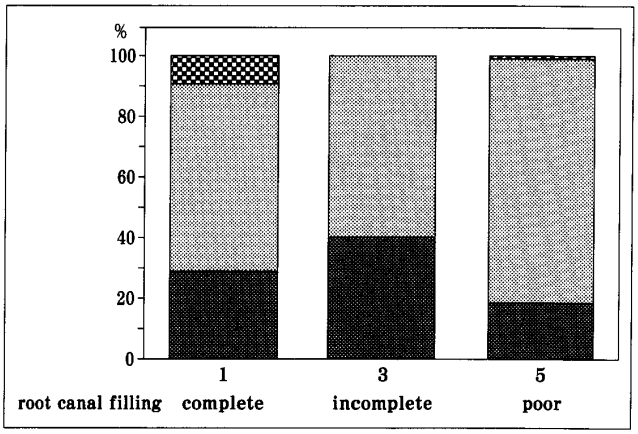

Fig. 7-3 Evaluation of Bone Changes by Z-score due to the Condition of Canal Filling

into below -2, between -2 and 2, and over 2 .

Lytic bone changes at the root apex were found in 17.4% by film findings and in 5.6% by Z-score. However, condensing osteitis was found in 46.3% on macroscopic findings, and in 35.5% by Z-score (Fig.7-2). These differences are considered due to a differences in the base density of the film causing evaluations of macroscopic findings from each other. Next, the relation to the condition of root canal fillings was examined to determine whether the condition of the root canal filling influenced the surrounding periapical bone. Radiograms were divided into 3 groups consisting of the complete root canal filling, the incomplete filling and the poor root canal filling based on the condition of the root canal filling. The results showed no relation to the condition of the root canal filling in this series. Since there are many factors that influence bone changes such as time course after fillings, there dose not seem to be any simple conclusion (Fig.7-3).

B. Evaluation of bone changes of around implants[11]

Implants have become common in dentistry and are now often performed. It is important to evaluate bone changes between the implant and its peripheral bone structure, which were used by radiograms. Here, bone changes caused by Biocerum and titanium were examined. Furthermore, progression of bone changes due to titanium were observed over 3 years (Fig.8-1, 2, 3). Al equivalent value and SD over time demonstrated bone changes due to Biocerum and titanium implants.

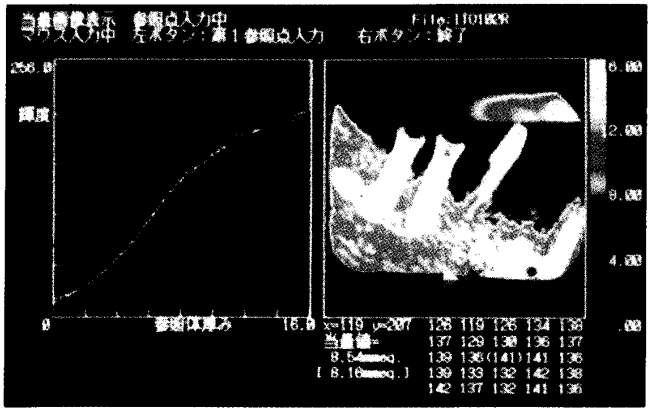

Fig. 8-1 Immediately after implant

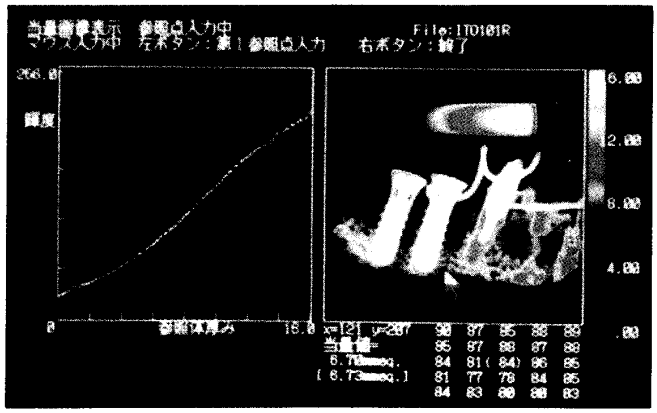

Fig. 8-2 3weeks after implant

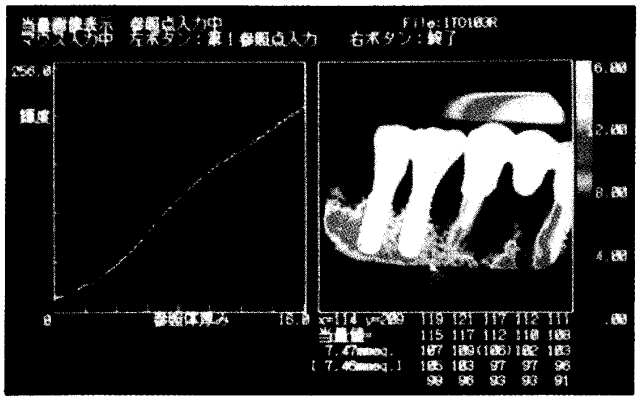

Fig. 8-3 6 month after implant

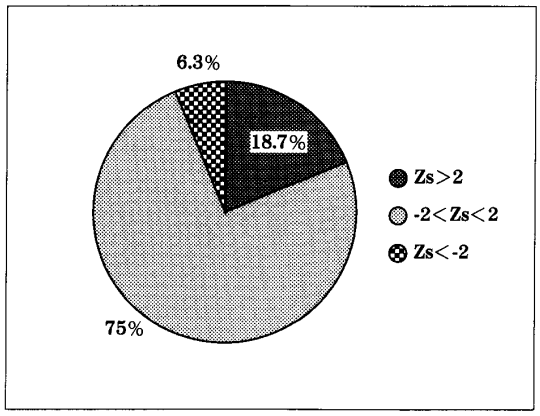

Fig. 8-4 Evaluation of Bone Changes with Titanium after 3 years by Z-score

Bone reaction was highest at about one year for Biocerum, while that for titanium occurred at about 6 months. Bone reaction seemed to occur earlier with titanium than with Biocerum. Bone changes around a titanium implant over 3 years were shown as the ratio to Al equivalent value. As the evaluation by Z-score at 3 years after implant, the normal level was estimated to be 75%, and sclerosing osteitis 18.7%, while bone resorption was 6.3% (Fig.8-4).

C. Evaluation of mandibular bone changes in elderly subjects

Human longevity is currently increasing and osteoporosis in females is especially becoming issue. Osteoporosis of the mandible was examined by Z-score. The elderly group consisted of 17 males and 39 females with average ages of 76.7 and 81 years, respectively. In the edentulous mandibular bone, the sampling area was set at the mental foramen as a standard point (Fig.9-1). Approximately 31% of the female group was thought to show osteoporosis in the mandible (Fig.9-2).

D. Evaluation of mandibular bone changes of ESRD

End stage renal diseases (ESRD) are known to cause bone changes not only in skeletal bone but also in the maxilla and mandible[12, 13, 14]. Over time, abnormal bone formation occurred in the maxilla during prolonged hemodialysis. The panoramic radiogram showed destructive enlargement and mixed radiolucent and radiopaque findings in the maxilla and mandible. The histologic findings demonstrated new bone formations arranged in parallel, while, loss of cortical bone and

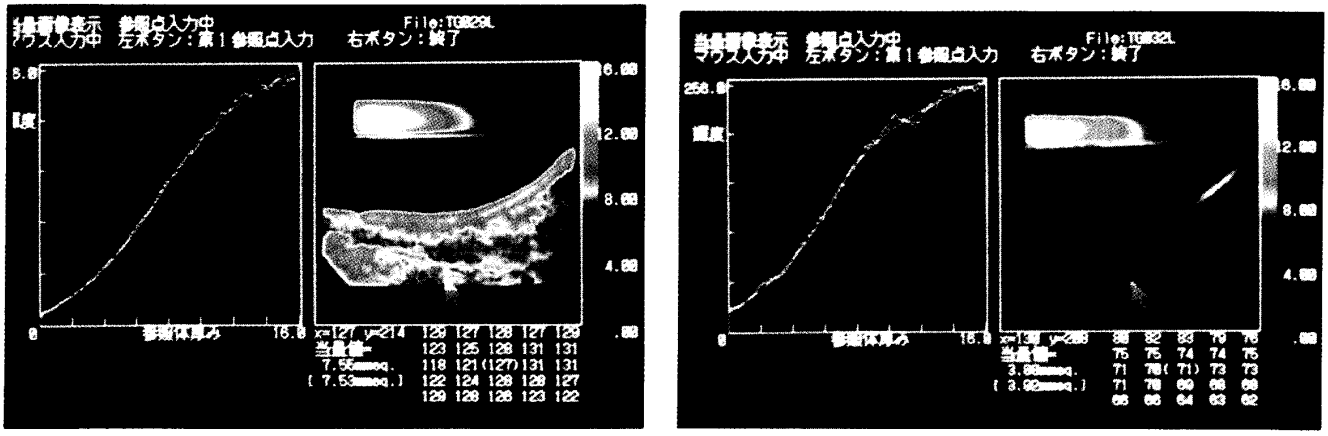

Fig. 9-1 Evaluation of mandibular Bone Changes in elder subjects.
83 years old, man. 85 years old, woman.

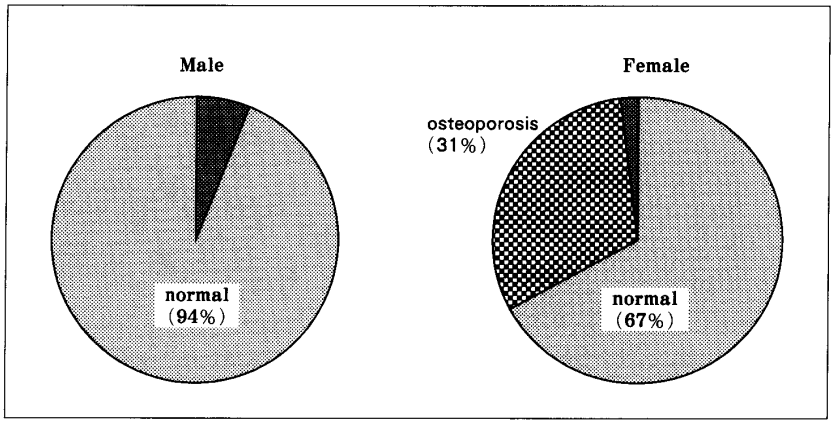

Fig. 9-2 Mandibular Bone Change in Old Age Group

disappearance of trabecular bone were also observed, and both condyles were destroyed. Dental radiogram also showed the disappearance of lamina dura and a ground glass appearance was indicated. These finding seemed typical of secondary hyperparathyroidism. In this study, two hundred and ten (119 males and 91 females) chronic hemodialysis patients were investigated. Patient ages ranged from 27 to 83 years with an average of 55.2 years in males and from 26 to 81 years with an average of 50.6 years in females. The duration of hemodialysis treatment ranged from 0.1 to 15 (average 5.8) years. The hemodialysis patients were divided into 3 groups by the level of serum I-PTH; group A: hyperparathyroidism (>300pg/ml), group B: normal (100<I-PTH<300pg/ml), group C: hypoparathyroidism (<100pg/ml) (Fig. 10-1). Correlation among BMC and serum biochemical variables was estimated in each group. According to this classification, there were 11 (5.2%) in the hyperparathyroidism group, 26 (12.4%) in the normal group and 173 (82.4%) in the hypoparathyroidism group (Fig.10-2). Correlation between factors of bone metabolism such as Z-score and serum biochemical factors in all hemodialysis patients was summarized (Fig.10-3). Then we focused in the relationship among Z-score, I-PTH, I-BGP and $1,25(OH)_2D_3$ in each 3 groups. In the hyperparathyroidism group, there was an inverse correlation between Z-score and PTH ($r=-0.438$) or BGP level ($r=-0.274$) (Fig.10-4, 5). As PTH and BGP increased, the Z-score decreased. However, there was no correlation between Z-score and PTH in the hypoparathyroidism group. The

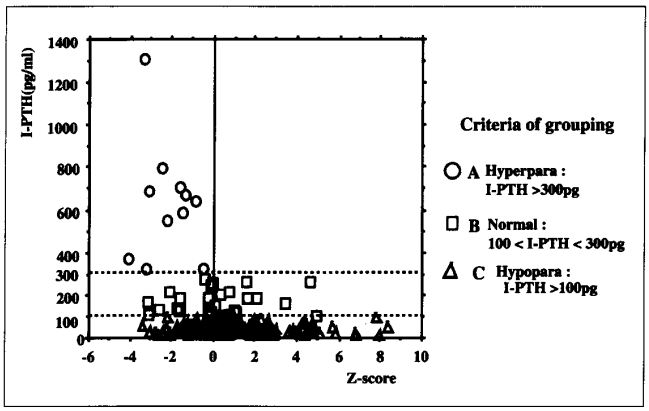

Fig. 10-1 Scattergram according to Z-score and I-PTH

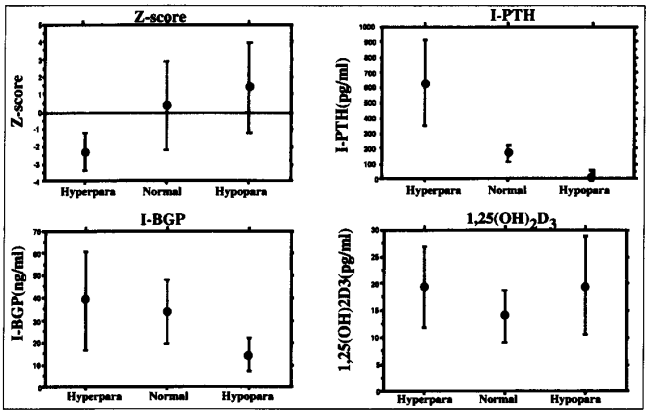

Fig. 10-2 Average and SD of Z-score, I-PTH, BGP and $1,25(OH)_2D_3$ in each groups

	Z-score	I-PTH	Hs-PTH	I-BGP	ALP	1,25VD3	Ca	P
Z-score	1							
I-PTH	*-0.337	1						
Hs-PTH	*-0.297	*0.638	1					
I-BGP	*-0.369	*0.503	0.788	1				
ALP	-0.139	*0.161	0.130	*0.467	1			
1,25VD3	-0.031	-0.123		-0.027	-0.007	1		
Ca	-0.008	*-0.316	*-0.341	-0.208	*-0.215	0.160	1	
P	-0.118	*0.233	*0.451	0.120	0.016	-0.159	*-0.179	1

*P<0,05

Fig. 10-3 Correlation Matrix for Variables

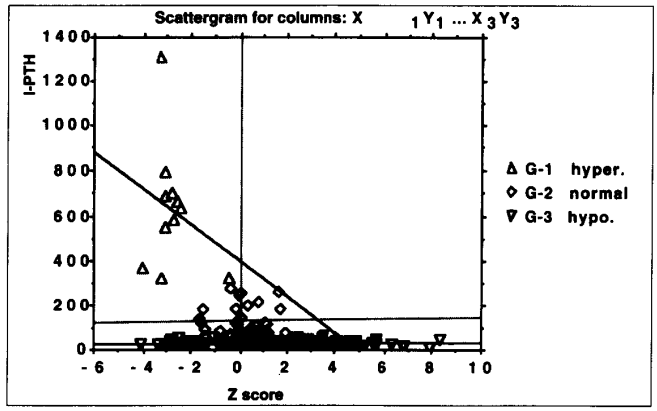

Fig. 10-4 Relation between Z-score and I-PTH in the Group

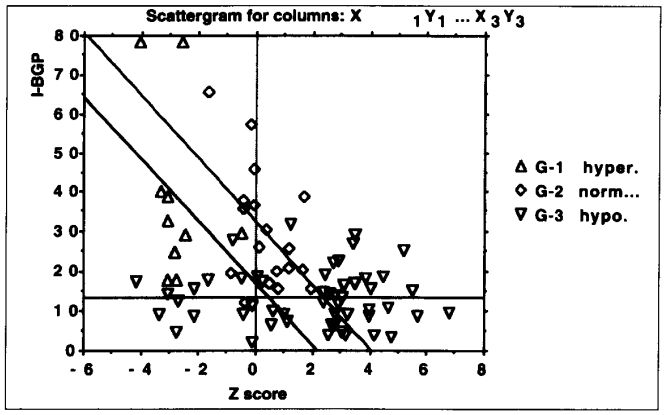

Fig. 10-5 Relation between Z-score and I-BGP in the Group

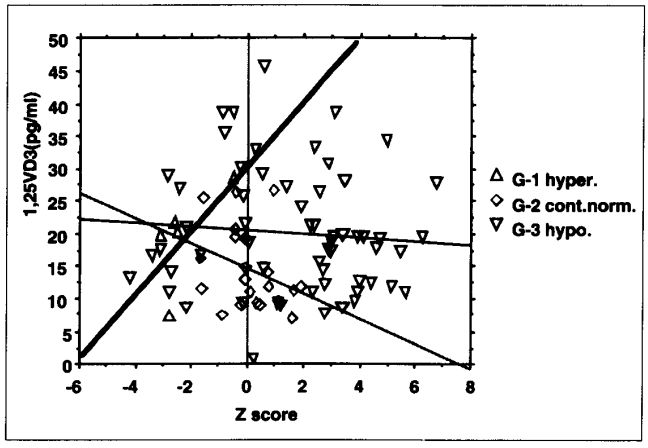

Fig. 10-6 Relation between Z-score and $1,25VD_3$ in the Group

BGP level was within normal range but did not correlate with the Z-score. The serum 1, $25(OH)_2D_3$ level was below the normal range in the hemodialyzed group. A positive correlation was found between Z-score and 1, $25(OH)_2D_3$ in the hyperparathyroidism group ($r=0.67$, $p<0.01$), (Fig.10-6), but there was no correlation in the hypoparathyroidism group.

IV. Application for animal experiments

A. The Effect of Microgravity to the Vertebral Growth in Growing Rats[15, 16, 17]

The effect of 14 days spaceflight on the vertebrae of rapidly growing rats was studied. Bone mineral density was measured from X-ray photographs (Fig.11-1), and the hardness of the vertebrae was measured with a Knoop microhardness tester. Histomorphometric examination was performed with a microcomputer aided system.

Twenty-five male Sprague-Dawley rats (8 week old) were used in this study. They were randomly assigned to the following five groups of five rats each: group A consisted of preflight ground control rats that were killed 2 h before launch; group B was made up of in-flight rats killed up to 5 h after landing; group C was the synchronous ground control of group B; group D was 14 days spaceflight rats which were killed 9 days after landing; group E was synchronous ground control of group D (One of a series of articles that describes research conducted on dedicated life sciences missions flown on the US space shuttle). In respect of bone mineral content ($CaCO_3$ mg/cm^2) by Equivalent images , there is no significant difference between flight group (B, C) and synchronous group (B, D), (Fig.11-2). On project direction, significant correlation was observed between vertical and horizontal in the synchronous group(C, E), but in the flight group (B, D) there was disappeared in its relationship. Max length per a trabecule by Particle analysis showed tendency to shortening in group B, but in the group D which lived on the ground in 9 days after space flight,

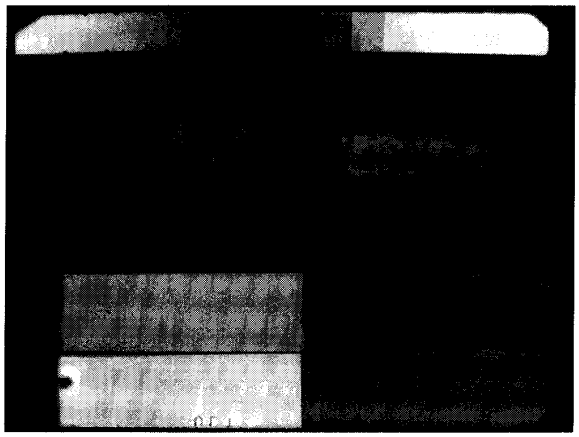

Fig. 11-1 X-ray image of vertebre

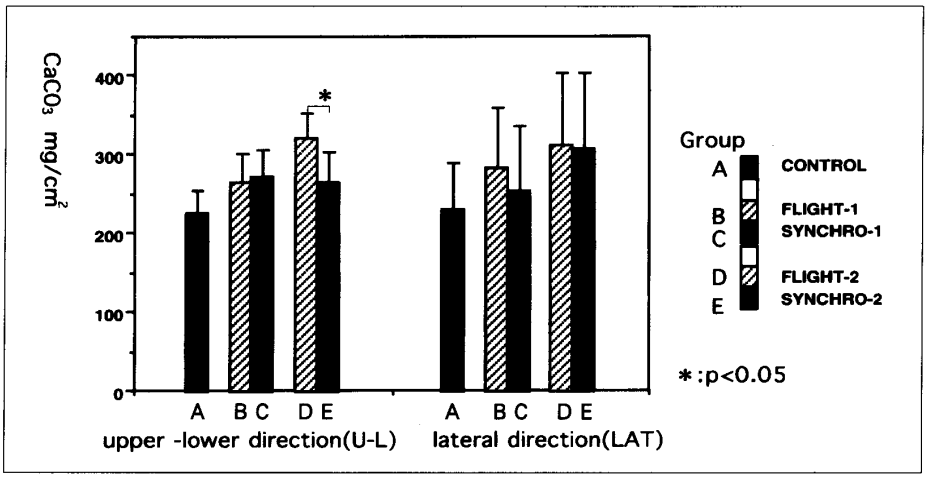

Fig. 11-2 Bone mineral content (Thoratic bone 3-10)

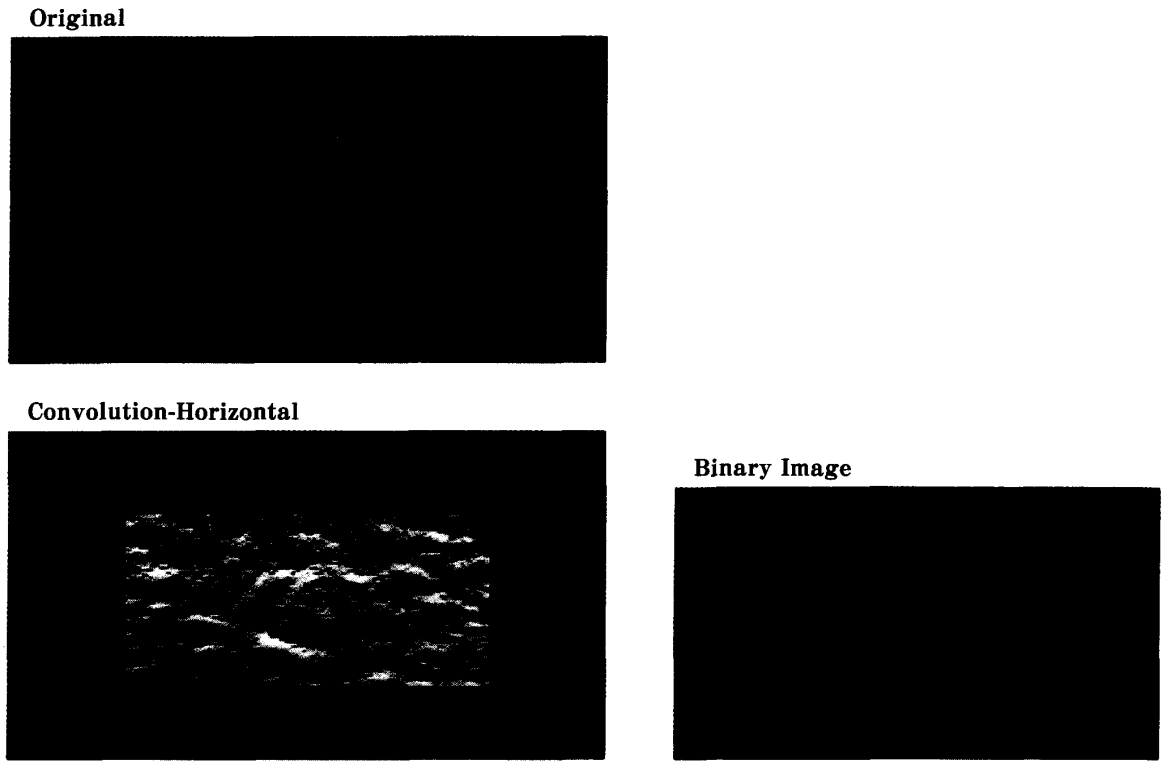

Fig. 11-3 Particle Analysis of trabecular bone

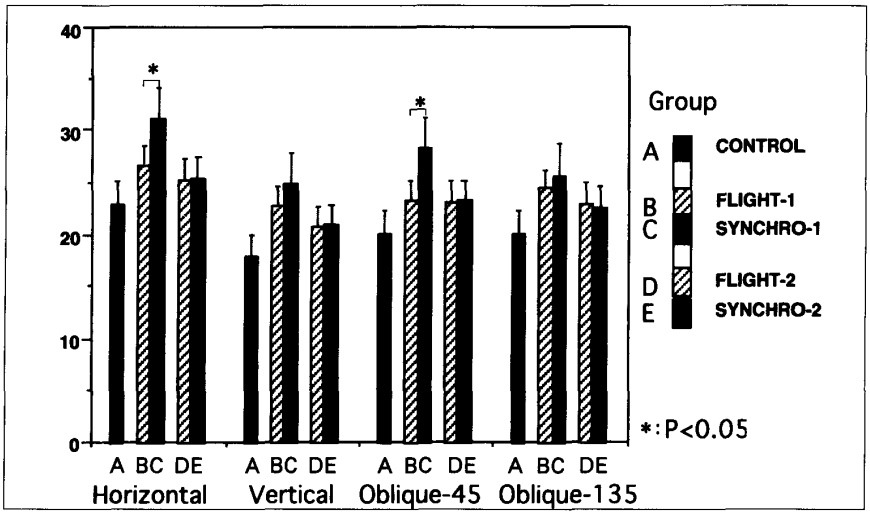

Fig. 11-4 Detected max length of trabecular bone (Th8 and 9)

they were become in same group E (Fig.11-3, 4). It was suggested recovery. Fractal dimension showed no difference between flight group and synchronous group. Hardness by Knoop test showed also no difference between flight group and synchronous group. In histomorphometry, there found irregular and thick immature cortical bone, and decreased formation of lammellated bone (Fig.11-5).

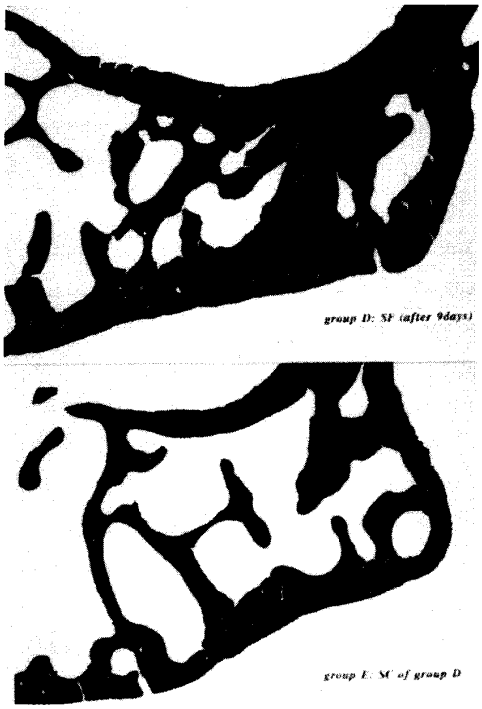

Fig. 11-5 Pathological finding upper control rat bottom flight rat

B. Effects on the bone mineral content by hindlimb suspension in rats[19]

An experiment simulating a microgravity condition during space flight was performed by Professor Ohira of the National Institute of Fitness and Sports, Kanoya by suspending the tail of rats and relieving the hind legs from the body weight (Fig.12-1). The bone mineral content of the femur was measured in rats after 14-day suspension of the hind legs, which was the same duration as the 1993 flight of the NASA space shuttle Columbia (STS-58), and rats after 14 day suspension of hind legs followed by 23-day normal rearing. The bone mineral content was decreased after 14-day suspension of the hind legs compared with controls, but it tended to recover after 23-day normal life; the results were similar to those under the microgravity condition of space flight (Fig.12-2).

In summary, This Al-equivalent images was able to demonstrate not the absolutely quantity of bone mineral content, but relative changes. This

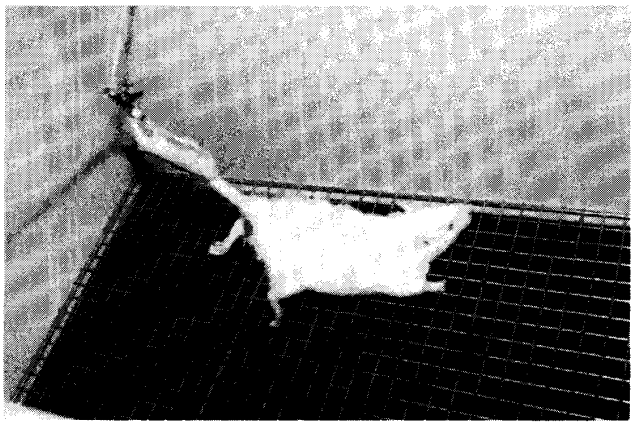

Fig. 12-1 Tail Suspension of Rat

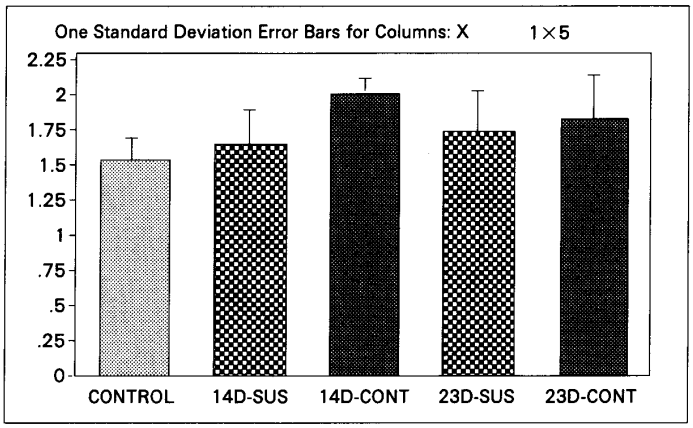

Fig. 12-2 Bone mineral content of femur

method can easily measure bone mineral content of mandibular bone, and evaluate various kinds of lesions. Furthermore, it is used for bone changes of experimental animals.

Reference

1) Kalender, W. A., Felsenberg, D., Louis, O., Loopez, P., Klotz, E., Osteaux, M. and Fraga, J.: Reference values for trabecular and cortical vertebral bone density in single and dual-energy quantitative computed tomography. Europ. J. Radiol., 9 : 75-80, 1989.
2) Hagiwara, S., Miki, T., Nishizawa, Y., Ochi, H. and Mori, H.: Quantification of bone mineral contents using dual photonabsorptiometry in a normal japanese population. JBMM, 9 : 263-269, 1991.
3) Griffith, E. R., Stonebridge, J. B., Piernick, D. and Lehman, J. F.: Development of a method of X-ray densitometory for bone mineral measurment. Am J Roentogenol., 52 : 128-149, 1973.
4) Trouerbach W., Hoornstra K. and Zwamborn A. W.: Microdensitometric analysis of interdental bone structure. Dentomaxillofac. Radiol., 13 : 27-31, 1984.
5) Iwashita Y., Morita Y, and Norikura T. : Al-equivalent image of intra oral radiograms. J. Dent. Radiol. 29 : 289-294, 1989.
6) Nervig P., Wing K., Welander U.: Sens-A-Ray: A new system for direct digital intraoral radiography. Oral Surg Oral Med Oral Pathol, 76 : 235-243, 1993.
7) Welander U., Nelvig P., Tronje G. et al.: Basic technical properties of a system for direct acquisition of digital intraoral radiographs. Oral Surg Oral Med Oral Pathol, 75 : 506-516, 1993.
8) Ishigaki T., Sakuma S., Horikawa Y., Ikeda M., Yamaguchi H.: One-shot dual-energy subtraction imaging. Radiology. 161 : 271-273, 1986.
9) Stewart B. K., Huang H. K.: Single-exposure dual-energy computed radiography. Med Phys.; 17 : 866-875, 1990.
10) Ito W., Shimura K., Nakajima N., Ishida M., Kato H.: Improvement of detection in computed radiography by new single-exposure dual-energy subtraction. SPIE Medical Imaging VI (Image Processing).; 1652 : 368-395, 1992.
11) Takeda H., Itoh T., Takaki K., Nishimura K., Noikura T. and Oku R.: Radiological Observation of Implants by Means of AL-equivalent Images, 6(2), 323-326, 1993.
12) Rickers, H., Nielsen, A. H., Pedersen, R. S., Rodbro, P.: Bone Mineral Loss during Maintenance Hemodialysis. Acta Med Scand, 204 : 263-267, 1978.
13) Kelly, W. H., Mirahmadi, M. K., Simon, J. H. and Gorman, J. T.: Radiographic changes of the jaw bones in end stage renal disease. Oral Surg, 50 : 372-381, 1980.
14) Bras, J., Ooij, C. P., Abraham-Inpijin, L., Wilmink, J. M. and Kusen, G. J.: Radiographic interpretation of the mandibular angular cortex. Oral Surg, 53 : 647-650, 1982.
15) Morey, E. R., and D. J. Baylink. Inhibition of bone formation during space flight. Science. Wash. DC 201 : 1138-1141, 1978.
16) Jee, W. S. S., T. J. Wronski, E. R. Morey, and D. B. Kimmel. Effects of spaceflight on trabecular bone in rats. Am. J. Physiol. 244 : R310-R314, 1983.
17) Vailas, A. C., R. F. Zernicke, R. E. Grindeland, A. Kaplansky, G. N. Durnova, K. -C. Li, and D. A. Martinez. Effects of space-flight on rat humerus geometry, biomechanics and biochemistry. FASEB J. 4 : 47-54, 1990.
18) Kitajima, I., Semba, I., Noikura, T., et al. Vertebral growth disturbance in rapidly growing rats during 14 days of spaceflight. J Appl. Physiol.; 81 : 156-163, 1996.
19) Osako, T., Y. Ohira, G. Ito, Y. Iwashita, T. Norikura, and E. Maki. Structure and mineral content in weight-bearing bones following hind limb suspension in young rats. Jpn. J, Physiol. 41 : 923-932, 1991.